Measurements of Elliptic and Triangular Flow in High-Multiplicity He3+Au Collisions at √sNN=200 GeV

(PHENIX Collaboration) Adare, A.; ...; Makek, Mihael; ...; Zou, L.

Measurements of Elliptic and Triangular Flow in High-Multiplicity ^{3}He + Au Collisions at $\sqrt{s_{NN}} = 200$ GeV

A. Adare,[14] S. Afanasiev,[33] C. Aidala,[15,42,46,47] N. N. Ajitanand,[66] Y. Akiba,[60,61] R. Akimoto,[13] H. Al-Bataineh,[54] J. Alexander,[66] M. Alfred,[26] H. Al-Ta'ani,[54] K. R. Andrews,[1] A. Angerami,[15] K. Aoki,[35,38,60] N. Apadula,[31,67] L. Aphecetche,[68] E. Appelt,[72] Y. Aramaki,[13,60] R. Armendariz,[9,54] S. H. Aronson,[8] J. Asai,[60,61] H. Asano,[38,60] E. C. Aschenauer,[8] E. T. Atomssa,[39,67] R. Averbeck,[67] T. C. Awes,[56] B. Azmoun,[8] V. Babintsev,[27] M. Bai,[7] G. Baksay,[21] L. Baksay,[21] A. Baldisseri,[17] N. S. Bandara,[46] B. Bannier,[67] K. N. Barish,[9] P. D. Barnes,[42,*] B. Bassalleck,[53] A. T. Basye,[1] S. Bathe,[6,9,61] S. Batsouli,[56] V. Baublis,[59] C. Baumann,[8,48] A. Bazilevsky,[8] M. Beaumier,[9] S. Beckman,[14] S. Belikov,[8,*] R. Belmont,[14,47,72] J. Ben-Benjamin,[49] R. Bennett,[67] A. Berdnikov,[63] Y. Berdnikov,[63] J. H. Bhom,[76] A. A. Bickley,[14] D. S. Blau,[37] J. G. Boissevain,[42] J. S. Bok,[54,76] H. Borel,[17] K. Boyle,[61,67] M. L. Brooks,[42] D. Broxmeyer,[49] J. Bryslawskyj,[6] H. Buesching,[8] V. Bumazhnov,[27] G. Bunce,[8,61] S. Butsyk,[42,67] C. M. Camacho,[42] S. Campbell,[15,31,67] A. Caringi,[49] P. Castera,[67] B. S. Chang,[76] W. C. Chang,[2] J.-L. Charvet,[17] C.-H. Chen,[61,67] S. Chernichenko,[27] C. Y. Chi,[15] J. Chiba,[35] M. Chiu,[8,28] I. J. Choi,[28,76] J. B. Choi,[11] R. K. Choudhury,[5] P. Christiansen,[44] T. Chujo,[71,72] P. Chung,[66] A. Churyn,[27] O. Chvala,[9] V. Cianciolo,[56] Z. Citron,[67,74] C. R. Cleven,[23] B. A. Cole,[15] M. P. Comets,[57] Z. Conesa del Valle,[39] M. Connors,[67] P. Constantin,[42] M. Csanád,[19] T. Csörgő,[75] T. Dahms,[67] S. Dairaku,[38,60] I. Danchev,[72] D. Danley,[55] K. Das,[22] A. Datta,[46,53] M. S. Daugherity,[1] G. David,[8] M. K. Dayananda,[23] M. B. Deaton,[1] K. DeBlasio,[53] K. Dehmelt,[21,67] H. Delagrange,[68,*] A. Denisov,[27] D. d'Enterria,[15,39] A. Deshpande,[61,67] E. J. Desmond,[8] K. V. Dharmawardane,[54] O. Dietzsch,[64] A. Dion,[31,67] P. B. Diss,[45] J. H. Do,[76] M. Donadelli,[64] L. D'Orazio,[45] O. Drapier,[39] A. Drees,[67] K. A. Drees,[7] A. K. Dubey,[74] J. M. Durham,[42,67] A. Durum,[27] D. Dutta,[5] V. Dzhordzhadze,[9] S. Edwards,[7,22] Y. V. Efremenko,[56] J. Egdemir,[67] F. Ellinghaus,[14] W. S. Emam,[9] T. Engelmore,[15] A. Enokizono,[41,56,60,62] H. En'yo,[60,61] S. Esumi,[71] K. O. Eyser,[8,9] B. Fadem,[49] N. Feege,[67] D. E. Fields,[53,61] M. Finger,[10,33] M. Finger, Jr.,[10,33] F. Fleuret,[39] S. L. Fokin,[37] Z. Fraenkel,[74,*] J. E. Frantz,[55,67] A. Franz,[8] A. D. Frawley,[22] K. Fujiwara,[60] Y. Fukao,[38,60] T. Fusayasu,[51] S. Gadrat,[43] C. Gal,[67] P. Gallus,[16] P. Garg,[4] I. Garishvili,[41,69] H. Ge,[67] F. Giordano,[28] A. Glenn,[14,41] H. Gong,[67] X. Gong,[66] M. Gonin,[39] J. Gosset,[17] Y. Goto,[60,61] R. Granier de Cassagnac,[39] N. Grau,[3,15,31] S. V. Greene,[72] G. Grim,[42] M. Grosse Perdekamp,[28,61] Y. Gu,[67] T. Gunji,[13] L. Guo,[42] H.-Å. Gustafsson,[44,*] T. Hachiya,[25,60] A. Hadj Henni,[68] C. Haegemann,[53] J. S. Haggerty,[8] K. I. Hahn,[20] H. Hamagaki,[13] J. Hamblen,[69] H. F. Hamilton,[1] R. Han,[58] S. Y. Han,[20] J. Hanks,[15,67] H. Harada,[25] C. Harper,[49] E. P. Hartouni,[41] K. Haruna,[25] S. Hasegawa,[32] T. O. S. Haseler,[23] K. Hashimoto,[60,62] E. Haslum,[44] R. Hayano,[13] X. He,[23] M. Heffner,[41] T. K. Hemmick,[67] T. Hester,[9] H. Hiejima,[28] J. C. Hill,[31] R. Hobbs,[53] M. Hohlmann,[21] R. S. Hollis,[9] W. Holzmann,[15,66] K. Homma,[25] B. Hong,[36] T. Horaguchi,[13,25,60,70,71] Y. Hori,[13] D. Hornback,[56,69] T. Hoshino,[25] N. Hotvedt,[31] J. Huang,[8] S. Huang,[72] T. Ichihara,[60,61] R. Ichimiya,[60] H. Iinuma,[35,38,60] Y. Ikeda,[71] K. Imai,[32,38,60] J. Imrek,[18] M. Inaba,[71] Y. Inoue,[60,62] A. Iordanova,[9] D. Isenhower,[1] L. Isenhower,[1] M. Ishihara,[60] T. Isobe,[13,60] M. Issah,[66,72] A. Isupov,[33] D. Ivanishchev,[59] Y. Iwanaga,[25] B. V. Jacak,[67] M. Jezghani,[23] J. Jia,[8,15,66] X. Jiang,[42] J. Jin,[15] O. Jinnouchi,[61] D. John,[69] B. M. Johnson,[8] T. Jones,[1] K. S. Joo,[50] D. Jouan,[57] D. S. Jumper,[1,28] F. Kajihara,[13] S. Kametani,[13,60,73] N. Kamihara,[60,61] J. Kamin,[67] S. Kanda,[13] M. Kaneta,[61] S. Kaneti,[67] B. H. Kang,[24] J. H. Kang,[76] J. S. Kang,[24] H. Kanou,[60,70] J. Kapustinsky,[42] K. Karatsu,[38,60] M. Kasai,[60,62] D. Kawall,[46,61] M. Kawashima,[60,62] A. V. Kazantsev,[37] T. Kempel,[31] J. A. Key,[53] V. Khachatryan,[67] A. Khanzadeev,[59] K. M. Kijima,[25] J. Kikuchi,[73] A. Kim,[20] B. I. Kim,[36] C. Kim,[36] D. H. Kim,[50] D. J. Kim,[34,76] E. Kim,[65] E.-J. Kim,[11] G. W. Kim,[20] M. Kim,[65] S. H. Kim,[76] Y.-J. Kim,[28] Y. K. Kim,[24] B. Kimelman,[49] E. Kinney,[14] K. Kiriluk,[14] Á. Kiss,[19] E. Kistenev,[8] R. Kitamura,[13] A. Kiyomichi,[60] J. Klatsky,[22] J. Klay,[41] C. Klein-Boesing,[48] D. Kleinjan,[9] P. Kline,[67] T. Koblesky,[14] L. Kochenda,[59] V. Kochetkov,[27] B. Komkov,[59] M. Konno,[71] J. Koster,[28] D. Kotchetkov,[9,55] D. Kotov,[59,63] A. Kozlov,[74] A. Král,[16] A. Kravitz,[15] J. Kubart,[10,30] G. J. Kunde,[42] N. Kurihara,[13] K. Kurita,[60,62] M. Kurosawa,[60,61] M. J. Kweon,[36] Y. Kwon,[69,76] G. S. Kyle,[54] R. Lacey,[66] Y. S. Lai,[15] J. G. Lajoie,[31] D. Layton,[28] A. Lebedev,[31] D. M. Lee,[42] J. Lee,[20] K. B. Lee,[36] K. S. Lee,[36] M. K. Lee,[76] S. Lee,[76] S. H. Lee,[67] S. R. Lee,[11] T. Lee,[65] M. J. Leitch,[42] M. A. L. Leite,[64] B. Lenzi,[64] X. Li,[12] P. Lichtenwalner,[49] P. Liebing,[61] S. H. Lim,[76] L. A. Linden Levy,[14] T. Liška,[16] A. Litvinenko,[33] H. Liu,[42,54] M. X. Liu,[42] B. Love,[72] D. Lynch,[8] C. F. Maguire,[72] Y. I. Makdisi,[7] M. Makek,[77] A. Malakhov,[33] M. D. Malik,[53] A. Manion,[67] V. I. Manko,[37] E. Mannel,[8,15] Y. Mao,[58,60] L. Mašek,[10,30] H. Masui,[71] F. Matathias,[15] M. McCumber,[14,42,67] P. L. McGaughey,[42] D. McGlinchey,[14,22] C. McKinney,[28] N. Means,[67] A. Meles,[54] M. Mendoza,[9] B. Meredith,[28] Y. Miake,[71] T. Mibe,[35] A. C. Mignerey,[45] P. Mikeš,[10,30] K. Miki,[60,71] T. E. Miller,[72] A. Milov,[8,67,74] S. Mioduszewski,[8] D. K. Mishra,[5] M. Mishra,[4] J. T. Mitchell,[8] M. Mitrovski,[66] Y. Miyachi,[60,70] S. Miyasaka,[60,70] S. Mizuno,[60,71] A. K. Mohanty,[5] P. Montuenga,[28] H. J. Moon,[50] T. Moon,[76] Y. Morino,[13]

A. Morreale,[9] D. P. Morrison,[8†] S. Motschwiller,[49] T. V. Moukhanova,[37] D. Mukhopadhyay,[72] T. Murakami,[38,60] J. Murata,[60,62] A. Mwai,[66] S. Nagamiya,[35,60] K. Nagashima,[25] Y. Nagata,[71] J. L. Nagle,[14,‡] M. Naglis,[74] M. I. Nagy,[19,75] I. Nakagawa,[60,61] H. Nakagomi,[60,71] Y. Nakamiya,[25] K. R. Nakamura,[38,60] T. Nakamura,[25,60] K. Nakano,[60,70] S. Nam,[20] C. Nattrass,[69] P. K. Netrakanti,[5] J. Newby,[41] M. Nguyen,[67] M. Nihashi,[25] T. Niida,[71] S. Nishimura,[13] B. E. Norman,[42] R. Nouicer,[8,61] T. Novak,[75] N. Novitzky,[34,67] A. S. Nyanin,[37] C. Oakley,[23] E. O'Brien,[8] S. X. Oda,[13] C. A. Ogilvie,[31] H. Ohnishi,[60] M. Oka,[71] K. Okada,[61] O. O. Omiwade,[1] Y. Onuki,[60] J. D. Orjuela Koop,[14] J. D. Osborn,[47] A. Oskarsson,[44] M. Ouchida,[25,60] K. Ozawa,[13,35] R. Pak,[8] D. Pal,[72] A. P. T. Palounek,[42] V. Pantuev,[29,67] V. Papavassiliou,[54] B. H. Park,[24] I. H. Park,[20] J. Park,[65] J. S. Park,[65] S. Park,[65] S. K. Park,[36] W. J. Park,[36] S. F. Pate,[54] L. Patel,[23] M. Patel,[31] H. Pei,[31] J.-C. Peng,[28] H. Pereira,[17] D. V. Perepelitsa,[8] G. D. N. Perera,[54] V. Peresedov,[33] D. Yu. Peressounko,[37] J. Perry,[31] R. Petti,[8,67] C. Pinkenburg,[8] R. Pinson,[1] R. P. Pisani,[8] M. Proissl,[67] M. L. Purschke,[8] A. K. Purwar,[42] H. Qu,[23] J. Rak,[34,53] A. Rakotozafindrabe,[39] B. J. Ramson,[47] I. Ravinovich,[74] K. F. Read,[56,69] S. Rembeczki,[21] M. Reuter,[67] K. Reygers,[48] D. Reynolds,[66] V. Riabov,[52,59] Y. Riabov,[59,63] E. Richardson,[45] T. Rinn,[31] D. Roach,[72] G. Roche,[43,*] S. D. Rolnick,[9] A. Romana,[39,*] M. Rosati,[31] C. A. Rosen,[14] S. S. E. Rosendahl,[44] P. Rosnet,[43] Z. Rowan,[6] J. G. Rubin,[47] P. Rukoyatkin,[33] P. Ružička,[30] V. L. Rykov,[60] B. Sahlmueller,[48,67] N. Saito,[35,38,60,61] T. Sakaguchi,[8] S. Sakai,[71] K. Sakashita,[60,70] H. Sakata,[25] H. Sako,[32] V. Samsonov,[52,59] S. Sano,[13,73] M. Sarsour,[23] S. Sato,[32,35] T. Sato,[71] M. Savastio,[67] S. Sawada,[35] B. Schaefer,[72] B. K. Schmoll,[69] K. Sedgwick,[9] J. Seele,[14] R. Seidl,[28,60,61] A. Yu. Semenov,[31] V. Semenov,[27,29] A. Sen,[23,69] R. Seto,[9] P. Sett,[5] A. Sexton,[45] D. Sharma,[67,74] I. Shein,[27] A. Shevel,[59,66] T.-A. Shibata,[60,70] K. Shigaki,[25] H. H. Shim,[36] M. Shimomura,[31,71] K. Shoji,[38,60] P. Shukla,[5] A. Sickles,[8,28,67] C. L. Silva,[31,42,64] D. Silvermyr,[44,56] C. Silvestre,[17] K. S. Sim,[36] B. K. Singh,[4] C. P. Singh,[4] V. Singh,[4] S. Skutnik,[31] M. Slunečka,[10,33] M. Snowball,[42] T. Sodre,[49] A. Soldatov,[27] R. A. Soltz,[41] W. E. Sondheim,[42] S. P. Sorensen,[69] I. V. Sourikova,[8] F. Staley,[17] P. W. Stankus,[56] E. Stenlund,[44] M. Stepanov,[46,*] A. Ster,[75] S. P. Stoll,[8] T. Sugitate,[25] C. Suire,[57] A. Sukhanov,[8] T. Sumita,[60] J. Sun,[67] J. Sziklai,[75] T. Tabaru,[61] S. Takagi,[71] E. M. Takagui,[64] A. Takahara,[13] A. Taketani,[60,61] R. Tanabe,[71] Y. Tanaka,[51] S. Taneja,[67] K. Tanida,[38,60,61,65] M. J. Tannenbaum,[8] S. Tarafdar,[4,74] A. Taranenko,[52,66] P. Tarján,[18] E. Tennant,[54] H. Themann,[67] D. Thomas,[1] T. L. Thomas,[53] R. Tieulent,[23] A. Timilsina,[31] T. Todoroki,[60,71] M. Togawa,[38,60,61] A. Toia,[67] J. Tojo,[60] L. Tomášek,[30] M. Tomášek,[16,30] Y. Tomita,[71] H. Torii,[25,60] C. L. Towell,[1] R. Towell,[1] R. S. Towell,[1] V-N. Tram,[39] I. Tserruya,[74] Y. Tsuchimoto,[25] K. Utsunomiya,[13] C. Vale,[8,31] H. Valle,[72] H. W. van Hecke,[42] E. Vazquez-Zambrano,[15] A. Veicht,[15,28] J. Velkovska,[72] R. Vértesi,[18,75] A. A. Vinogradov,[37] M. Virius,[16] A. Vossen,[28] V. Vrba,[16,30] E. Vznuzdaev,[59] M. Wagner,[38,60] D. Walker,[67] X. R. Wang,[54,61] D. Watanabe,[25] K. Watanabe,[71] Y. Watanabe,[60,61] Y. S. Watanabe,[13,35] F. Wei,[31,54] R. Wei,[66] J. Wessels,[48] A. S. White,[47] S. N. White,[8] D. Winter,[15] C. L. Woody,[8] R. M. Wright,[1] M. Wysocki,[14,56] B. Xia,[55] W. Xie,[61] L. Xue,[23] S. Yalcin,[67] Y. L. Yamaguchi,[13,60,67,73] K. Yamaura,[25] R. Yang,[28] A. Yanovich,[27] Z. Yasin,[9] J. Ying,[23] S. Yokkaichi,[60,61] J. H. Yoo,[36] J. S. Yoo,[20] I. Yoon,[65] Z. You,[42,58] G. R. Young,[56] I. Younus,[40,53] H. Yu,[58] I. E. Yushmanov,[37] W. A. Zajc,[15] O. Zaudtke,[48] A. Zelenski,[7] C. Zhang,[56] S. Zhou,[12] J. Zimamyi,[75,*] L. Zolin,[33] and L. Zou[9]

(PHENIX Collaboration)

[1]*Abilene Christian University, Abilene, Texas 79699, USA*
[2]*Institute of Physics, Academia Sinica, Taipei 11529, Taiwan*
[3]*Department of Physics, Augustana University, Sioux Falls, South Dakota 57197, USA*
[4]*Department of Physics, Banaras Hindu University, Varanasi 221005, India*
[5]*Bhabha Atomic Research Centre, Bombay 400 085, India*
[6]*Baruch College, City University of New York, New York, New York 10010, USA*
[7]*Collider-Accelerator Department, Brookhaven National Laboratory, Upton, New York 11973-5000, USA*
[8]*Physics Department, Brookhaven National Laboratory, Upton, New York 11973-5000, USA*
[9]*University of California-Riverside, Riverside, California 92521, USA*
[10]*Charles University, Ovocný trh 5, Praha 1, 116 36 Prague, Czech Republic*
[11]*Chonbuk National University, Jeonju 561-756, Korea*
[12]*Science and Technology on Nuclear Data Laboratory, China Institute of Atomic Energy, Beijing 102413, People's Republic of China*
[13]*Center for Nuclear Study, Graduate School of Science, University of Tokyo, 7-3-1 Hongo, Bunkyo, Tokyo 113-0033, Japan*
[14]*University of Colorado, Boulder, Colorado 80309, USA*
[15]*Columbia University, New York, New York 10027, USA and Nevis Laboratories, Irvington, New York 10533, USA*
[16]*Czech Technical University, Zikova 4, 166 36 Prague 6, Czech Republic*

[17]Dapnia, CEA Saclay, F-91191 Gif-sur-Yvette, France
[18]Debrecen University, H-4010 Debrecen, Egyetem tér 1, Hungary
[19]ELTE, Eötvös Loránd University, H-1117 Budapest, Pázmány P. s. 1/A, Hungary
[20]Ewha Womans University, Seoul 120-750, Korea
[21]Florida Institute of Technology, Melbourne, Florida 32901, USA
[22]Florida State University, Tallahassee, Florida 32306, USA
[23]Georgia State University, Atlanta, Georgia 30303, USA
[24]Hanyang University, Seoul 133-792, Korea
[25]Hiroshima University, Kagamiyama, Higashi-Hiroshima 739-8526, Japan
[26]Department of Physics and Astronomy, Howard University, Washington, DC 20059, USA
[27]IHEP Protvino, State Research Center of Russian Federation, Institute for High Energy Physics, Protvino 142281, Russia
[28]University of Illinois at Urbana-Champaign, Urbana, Illinois 61801, USA
[29]Institute for Nuclear Research of the Russian Academy of Sciences, prospekt 60-letiya Oktyabrya 7a, Moscow 117312, Russia
[30]Institute of Physics, Academy of Sciences of the Czech Republic, Na Slovance 2, 182 21 Prague 8, Czech Republic
[31]Iowa State University, Ames, Iowa 50011, USA
[32]Advanced Science Research Center, Japan Atomic Energy Agency, 2-4 Shirakata Shirane, Tokai-mura, Naka-gun, Ibaraki-ken 319-1195, Japan
[33]Joint Institute for Nuclear Research, 141980 Dubna, Moscow Region, Russia
[34]Helsinki Institute of Physics and University of Jyväskylä, P.O.Box 35, FI-40014 Jyväskylä, Finland
[35]KEK, High Energy Accelerator Research Organization, Tsukuba, Ibaraki 305-0801, Japan
[36]Korea University, Seoul 136-701, Korea
[37]Russian Research Center "Kurchatov Institute", Moscow 123098, Russia
[38]Kyoto University, Kyoto 606-8502, Japan
[39]Laboratoire Leprince-Ringuet, Ecole Polytechnique, CNRS-IN2P3, Route de Saclay, F-91128 Palaiseau, France
[40]Physics Department, Lahore University of Management Sciences, Lahore 54792, Pakistan
[41]Lawrence Livermore National Laboratory, Livermore, California 94550, USA
[42]Los Alamos National Laboratory, Los Alamos, New Mexico 87545, USA
[43]LPC, Université Blaise Pascal, CNRS-IN2P3, Clermont-Fd, 63177 Aubiere Cedex, France
[44]Department of Physics, Lund University, Box 118, SE-221 00 Lund, Sweden
[45]University of Maryland, College Park, Maryland 20742, USA
[46]Department of Physics, University of Massachusetts, Amherst, Massachusetts 01003-9337, USA
[47]Department of Physics, University of Michigan, Ann Arbor, Michigan 48109-1040, USA
[48]Institut für Kernphysik, University of Muenster, D-48149 Muenster, Germany
[49]Muhlenberg College, Allentown, Pennsylvania 18104-5586, USA
[50]Myongji University, Yongin, Kyonggido 449-728, Korea
[51]Nagasaki Institute of Applied Science, Nagasaki-shi, Nagasaki 851-0193, Japan
[52]National Research Nuclear University, MEPhI, Moscow Engineering Physics Institute, Moscow 115409, Russia
[53]University of New Mexico, Albuquerque, New Mexico 87131, USA
[54]New Mexico State University, Las Cruces, New Mexico 88003, USA
[55]Department of Physics and Astronomy, Ohio University, Athens, Ohio 45701, USA
[56]Oak Ridge National Laboratory, Oak Ridge, Tennessee 37831, USA
[57]IPN-Orsay, Universite Paris Sud, CNRS-IN2P3, BP1, F-91406 Orsay, France
[58]Peking University, Beijing 100871, People's Republic of China
[59]PNPI, Petersburg Nuclear Physics Institute, Gatchina, Leningrad region 188300, Russia
[60]RIKEN Nishina Center for Accelerator-Based Science, Wako, Saitama 351-0198, Japan
[61]RIKEN BNL Research Center, Brookhaven National Laboratory, Upton, New York 11973-5000, USA
[62]Physics Department, Rikkyo University, 3-34-1 Nishi-Ikebukuro, Toshima, Tokyo 171-8501, Japan
[63]Saint Petersburg State Polytechnic University, St. Petersburg 195251, Russia
[64]Universidade de São Paulo, Instituto de Física, Caixa Postal 66318, São Paulo CEP05315-970, Brazil
[65]Department of Physics and Astronomy, Seoul National University, Seoul 151-742, Korea
[66]Chemistry Department, Stony Brook University, SUNY, Stony Brook, New York 11794-3400, USA
[67]Department of Physics and Astronomy, Stony Brook University, SUNY, Stony Brook, New York 11794-3800, USA
[68]SUBATECH (Ecole des Mines de Nantes, CNRS-IN2P3, Université de Nantes) BP 20722-44307 Nantes, France
[69]University of Tennessee, Knoxville, Tennessee 37996, USA
[70]Department of Physics, Tokyo Institute of Technology, Oh-okayama, Meguro, Tokyo 152-8551, Japan
[71]Center for Integrated Research in Fundamental Science and Engineering, University of Tsukuba, Tsukuba, Ibaraki 305, Japan
[72]Vanderbilt University, Nashville, Tennessee 37235, USA

[73]Waseda University, Advanced Research Institute for Science and Engineering, 17 Kikui-cho, Shinjuku-ku, Tokyo 162-0044, Japan
[74]Weizmann Institute, Rehovot 76100, Israel
[75]Institute for Particle and Nuclear Physics, Wigner Research Centre for Physics, Hungarian Academy of Sciences (Wigner RCP, RMKI) H-1525 Budapest 114, POBox 49, Budapest, Hungary
[76]Yonsei University, IPAP, Seoul 120-749, Korea
[77]University of Zagreb, Faculty of Science, Department of Physics, Bijenička 32, HR-10002 Zagreb, Croatia
(Received 22 July 2015; published 28 September 2015)

We present the first measurement of elliptic (v_2) and triangular (v_3) flow in high-multiplicity ^{3}He + Au collisions at $\sqrt{s_{NN}} = 200$ GeV. Two-particle correlations, where the particles have a large separation in pseudorapidity, are compared in ^{3}He + Au and in $p + p$ collisions and indicate that collective effects dominate the second and third Fourier components for the correlations observed in the ^{3}He + Au system. The collective behavior is quantified in terms of elliptic v_2 and triangular v_3 anisotropy coefficients measured with respect to their corresponding event planes. The v_2 values are comparable to those previously measured in $d + $ Au collisions at the same nucleon-nucleon center-of-mass energy. Comparisons with various theoretical predictions are made, including to models where the hot spots created by the impact of the three ^{3}He nucleons on the Au nucleus expand hydrodynamically to generate the triangular flow. The agreement of these models with data may indicate the formation of low-viscosity quark-gluon plasma even in these small collision systems.

DOI: 10.1103/PhysRevLett.115.142301 PACS numbers: 25.75.Dw

The study of high-energy heavy ion collisions at the Relativistic Heavy Ion Collider (RHIC) and the Large Hadron Collider has produced abundant evidence for the formation of quark-gluon plasma (QGP). Observation of strong elliptic and triangular flow in these $A + A$ collisions indicates that the QGP has a very small viscosity and behaves like a nearly perfect fluid [1–3]. Recently, measurements at the Large Hadron Collider in very high multiplicity events from collisions of $p + p$ and $p +$ Pb have revealed similar particle emission patterns [4–8]. Such features have also been detected in $d + $ Au collisions at RHIC [9–11]. Explanations of the data in terms of the formation of small droplets of QGP, which then expand hydrodynamically [12], compete with alternatives involving novel initial-state effects (e.g., glasma models [13]). RHIC is uniquely suited to test these competing theories by its ability to engineer the size and shape of the initial reaction zone through collisions of $p + $ Au, $d + $ Au, and ^{3}He + Au, as proposed in Ref. [14]. In the case when small QGP droplets are formed, the latter two systems should have the strongest elliptic and triangular flow patterns, respectively.

The azimuthal anisotropy of produced particles can be quantified by the Fourier coefficients v_n in the expansion of the particles' distribution as $dN/d\phi \propto 1 + \sum_{n=1} 2v_n \cos(n(\phi - \Psi_n))$ [15], where n is the order of the harmonic, ϕ is the azimuthal angle of particles of a given type, and Ψ_n is the azimuthal angle of the nth-order event plane. In this Letter, the elliptic (v_2) and triangular (v_3) flow for inclusive charged hadrons produced at midrapidity $|\eta| < 0.35$ in high-multiplicity ^{3}He + Au collisions at $\sqrt{s_{NN}} = 200$ GeV are measured in the PHENIX experiment with respect to Ψ_2 and Ψ_3 event planes. The signatures of collective motion beyond known nonflow correlation effects (e.g., jets, resonances, etc.) are also examined by comparing long-range correlations between ^{3}He + Au and $p + p$ collisions.

A full description of the PHENIX experimental setup is given in Ref. [16]. Charged particles are reconstructed in the two PHENIX central-arm tracking systems comprising drift chambers (DC) and multiwire proportional pad chambers (PC) [17]. Each arm covers $\pi/2$ in azimuth and $|\eta| < 0.35$. The DC tracks are matched to hits in the outermost PC layer (PC3), reducing the contribution of tracks originating from decays and photon conversions.

The observed event-plane angles Ψ_n^{Obs} are measured in different pseudorapidity ranges by the beam-beam counters [18] (BBC) and forward-silicon-vertex [19] (FVTX) detectors. The PHENIX experiment has two BBCs, each comprising 64 quartz Čerenkov radiators read out by photomultiplier tubes (PMTs), subtending pseudorapidity ($3.0 < |\eta| < 3.9$). The FVTX [19] detector comprises two identical end cap assemblies, located symmetrically in the north and south directions. Charged particles can be detected with a high efficiency ($>95\%$) using a cluster of ministrip hits. The event planes are measured by the BBC in the Au-going (south) direction (BBC-S), which covers $-3.9 < \eta < -3.0$, and by the reconstructed clusters in the FVTX in the Au-going (south) end cap (FVTX-S), which covers $-3.0 < \eta < -1.0$.

The ^{3}He + Au data for this analysis were obtained in the 2014 run of the PHENIX experiment and include 1.6 billion minimum-bias (MB) triggered events and 480 million high-multiplicity (HM) triggered events. The MB trigger is defined as a coincidence between the north and south BBCs requiring one or more photomultiplier tubes firing in each,

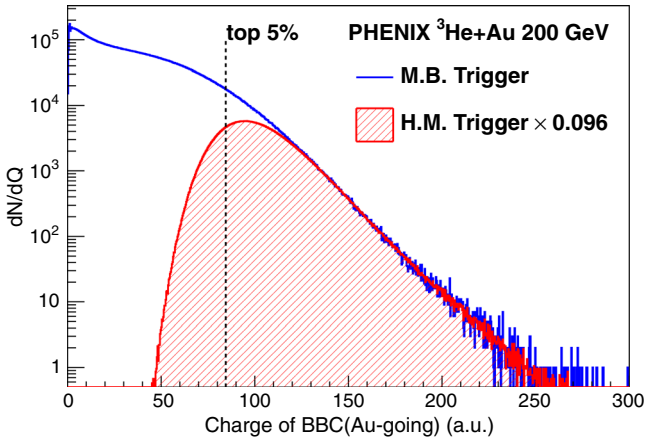

FIG. 1 (color online). The BBC-S charge distribution in minimum bias $^3\mathrm{He}+\mathrm{Au}$ events and in high-multiplicity triggered events, scaled appropriately. The dashed line indicates the threshold selecting the 0%–5% most central events.

capturing $88\pm4\%$ of the total inelastic $^3\mathrm{He}+\mathrm{Au}$ cross section. The HM trigger is based on the MB trigger, but additionally requires more than 48 photomultiplier tubes firing in the BBC-S.

The event centrality class in $^3\mathrm{He}+\mathrm{Au}$ collisions is determined as a percentile of the total charge $\sum Q^{\mathrm{BBC\text{-}S}}$ measured in the BBC-S [18,20–22]. The distribution of BBC-S PMT charge sum is shown in Fig. 1 for both MB and HM triggered events. The distribution for HM events has been scaled down by the relative online trigger prescale factor. For the MB sample, a threshold on the BBC-S charge sum shown in Fig. 1 is applied to select the top 5% central $^3\mathrm{He}+\mathrm{Au}$ collisions. In total, 400 million events have been used for the measurement of v_2 and v_3 including both HM and MB triggered events having BBC-S charge sum above the threshold.

Events with high BBC-S sum charge have been simulated with a Monte Carlo Glauber model [23,24], following the procedure detailed in Ref. [18]. The average number of binary collisions (N_{coll}), participants (N_{part}), and initial-state eccentricities (ε_2, ε_3) were found to be consistent, within uncertainties, between the MB with the 0%–5% central selection and the HM events being used here. Note that in this Glauber calculation, the spatial distribution from each participant is smeared with a two-dimensional Gaussian, $\sigma_r = 0.4$ fm [18]. The simulation results for central $^3\mathrm{He}+\mathrm{Au}$ and $d+\mathrm{Au}$ are listed in Table I with the $d+\mathrm{Au}$ values from Ref. [18].

TABLE I. Monte Carlo Glauber characterization results.

System	N_{part}	N_{coll}	ε_2	ε_3
0%–5% $^3\mathrm{He}+\mathrm{Au}$	25.0 ± 1.6	26.1 ± 2.0	0.50 ± 0.02	0.28 ± 0.02
0%–5% $d+\mathrm{Au}$	17.3 ± 1.2	18.1 ± 1.2	0.54 ± 0.04	0.19 ± 0.01

To estimate the contribution to the flow measurements from elementary processes, such as jets and resonance decay, we first examine azimuthal correlations in minimum bias $p+p$ and central $^3\mathrm{He}+\mathrm{Au}$ events across a long range in pseudorapidity, with $|\Delta\eta|\sim3.5$ between tracks in the PHENIX central arm at a given p_T and charge measured in the BBC PMTs. We use the BBCs for these correlation functions because the detector configuration and performance is uniform over many years, which enables us to combine data for $p+p$ collisions at $\sqrt{s}=200$ GeV from running in 2005, 2006, 2008, and 2009. This results in 2.7 billion total minimum bias $p+p$ events.

Using track-BBC pairs, we construct the distribution over relative azimuth, and from that the normalized correlation function:

$$S(\Delta\phi, p_T) = \frac{d(w_{\mathrm{PMT}} N^{\mathrm{track}(p_T)\text{-}\mathrm{PMT}}_{\mathrm{Same\ event}})}{d\Delta\phi}, \quad (1)$$

$$C(\Delta\phi, p_T) = \frac{S(\Delta\phi, p_T)}{M(\Delta\phi, p_T)} \frac{\int_0^{2\pi} M(\Delta\phi, p_T) d\Delta\phi}{\int_0^{2\pi} S(\Delta\phi, p_T) d\Delta\phi}. \quad (2)$$

The weighting w_{PMT} for each pair is taken as the PMT charge. The signal distribution S is over pairs in the same event; the mixed distribution M is over pairs from different events in the same event centrality and z vertex bin, and serves to correct for any nonuniformity in acceptance over $\Delta\phi$.

Figure 2 shows the correlation functions $C(\Delta\phi, p_T)$ for different p_T bins, for HM $^3\mathrm{He}+\mathrm{Au}$ collisions using BBC-S, as shown in panels (a)–(c), and minimum-bias $p+p$ collisions using both BBCs, as shown in panels (d)–(f). We analyze these shapes by fitting each $C(\Delta\phi, p_T)$ to a four-term Fourier cosine expansion, $f(\Delta\phi) = 1+\sum_{n=1}^{4} 2c_n(p_T)\cos(n\Delta\phi)$. The sum function and each individual cosine component are plotted in Fig. 2 for each distribution. Central $^3\mathrm{He}+\mathrm{Au}$ collisions show a clearly visible enhancement of near-side pairs, producing a local maximum in the distribution at $\Delta\phi\sim0$. In contrast, $p+p$ collisions can be described almost completely by the dipole term $\cos(\Delta\phi)$, as expected generically from back-to-back jets and transverse momentum conservation.

As in our $d+\mathrm{Au}$ analysis [10], we estimate quantitatively the correlation strength that would be observed in a class of $^3\mathrm{He}+\mathrm{Au}$ collisions purely from elementary processes, such as in $p+p$ collisions. Approximating the $^3\mathrm{He}+\mathrm{Au}$ collisions as superpositions of some number N of $p+p$ collisions, we would then expect the correlation strengths c_n from the superposition to be the same as in $p+p$, but diluted by a factor of $1/N$. We then approximate this dilution factor as simply the ratio of total charge observed in the BBC-S detector in $p+p$ versus $^3\mathrm{He}+\mathrm{Au}$:

$$c_n^{\mathrm{HeAu\ elementary}}(p_T) \simeq c_n^{p+p}(p_T) \frac{(\sum Q^{\mathrm{BBC\text{-}S}})_{p+p}}{(\sum Q^{\mathrm{BBC\text{-}S}})_{\mathrm{HeAu}}} \quad (3)$$

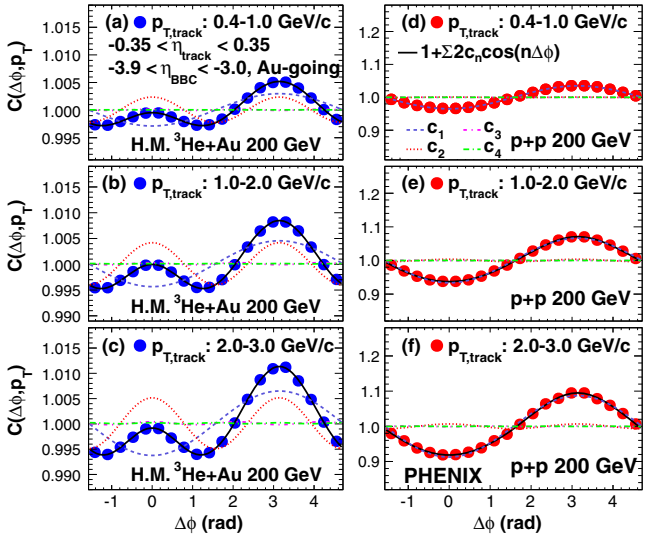

FIG. 2 (color online). The azimuthal correlation functions $C(\Delta\phi, p_T)$, as defined in Eq. (2), for track-BBC pairs with different track p_T selections in (a)–(c) HM $^3\mathrm{He} + \mathrm{Au}$ collisions and (d)–(f) minimum bias $p + p$ collisions both at $\sqrt{s_{NN}} = 200\,\mathrm{GeV}$. The track p_T bins are (a),(d) 0.4–1.0, (b),(e) 1.0–2.0, and (c),(f) 2.0–3.0 GeV/c. Each correlation function is fit with a four-term Fourier cosine expansion; the individual components $n = 1$ to $n = 4$ are drawn on each panel, together with the fit function sum.

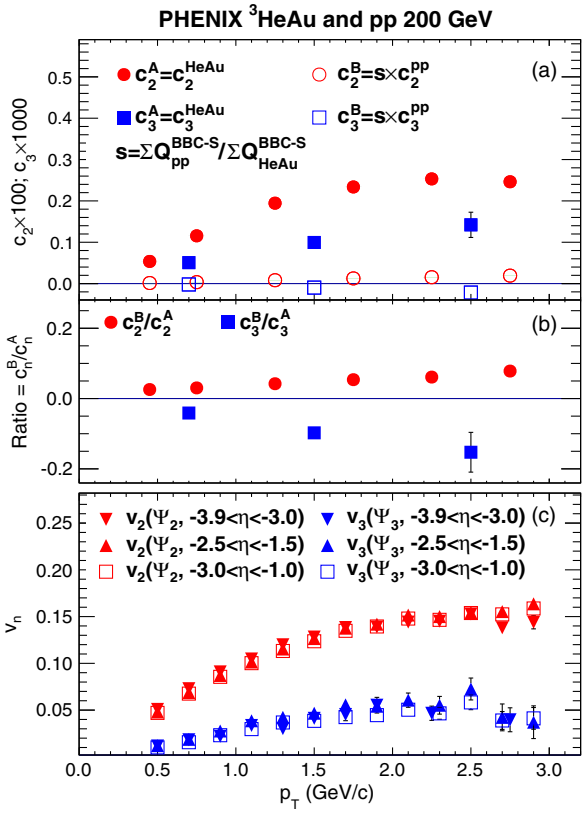

FIG. 3 (color online). (a) The $c_n(p_T)$ coefficients for track-BBC pairs from high multiplicity $^3\mathrm{He} + \mathrm{Au}$ collisions (filled, denoted "c^{A}") and $c_n(p_T)$ for pairs in minimum bias $p + p$ collisions times the dilution factor $(\sum Q^{\mathrm{BBC\text{-}S}})_{p+p}/(\sum Q^{\mathrm{BBC\text{-}S}})_{\mathrm{HeAu}}$ (open, denoted "c^{B}"). (b) The ratio $c^{\mathrm{B}}/c^{\mathrm{A}}$ is shown with statistical error bars. (c) Comparison of extracted values of v_2 and v_3 for midrapidity tracks in central $^3\mathrm{He} + \mathrm{Au}$ using event plane measurements with detectors in different pseudorapidity intervals (see text).

with a numerical value of $1/(20.6 \pm 0.4)$. Figure 3(a) shows the c_n's from the $^3\mathrm{He} + \mathrm{Au}$ correlation functions and from the $p + p$ with the dilution factor applied. The c_2^{pp} is found to be positive and the c_3^{pp} to be negative. This indicates that the correlation of elementary processes contributes positively to the v_2 but negatively to the v_3. The ratios in Fig. 3(b) show that the relative correlation strength in $^3\mathrm{He} + \mathrm{Au}$ from elementary processes grows with p_T, as might be expected from jet processes, for example, but does not exceed 7% (15%) for c_2 (c_3).

We now quantify the strength of collective behavior through the v_n coefficients. The v_n coefficients for charged hadrons at midrapidity are measured in central $^3\mathrm{He} + \mathrm{Au}$ events via the event-plane method [25] as $v_n(p_T) = \langle \cos n(\phi^{\mathrm{Particle}}(p_T) - \Psi_n^{\mathrm{Obs}}) \rangle / \mathrm{Res}(\Psi_n^{\mathrm{Obs}})$, where the average is over particles in the same p_T bin and events of the same centrality. The nth-order event-plane direction Ψ_n^{Obs} is determined in each event with the BBC-S or FVTX-S detectors. The Ψ_n^{Obs} are corrected for each detector with a standard event-plane flattening technique [25–28] to remove the effect of any small, residual nonuniformities in the detector response. As a cross-check, we use event planes from both the full FVTX-S covering $-3.0 < \eta < -1.0$ and a subsection covering $-2.5 < \eta < -1.5$. The choice of the latter is to avoid edge effects and still retain good FVTX-S acceptance.

We calculate the resolutions $\mathrm{Res}(\Psi_n^{\mathrm{Obs}})$ for each detector at each n using the standard three-event-plane method [10,25], combining two event planes with the nth order event plane determined from central-arm tracks, restricted to low p_T ($0.2 < p_T < 2.0$ GeV/c) to minimize contribution from jet fragments. In the case of the $n = 2$ event plane, the resolution is also estimated using the first-order event plane measured with spectator neutrons in the shower-maximum detector of the zero-degree calorimeter [28,29] on the Au-going side ($\eta < -6.5$). The values for the resolution obtained in both methods are found to be consistent within uncertainties.

The event plane resolutions for each detector and order are shown in Table II. The v_2 and v_3 measured using the

TABLE II. The resolution of nth-order event-plane angles measured by the BBC-S and FVTX-S detectors.

Subsystem	$\mathrm{Res}(\Psi_2^{\mathrm{Obs}})$	$\mathrm{Res}(\Psi_3^{\mathrm{Obs}})$
BBC-S ($-3.9 < \eta < -3.0$)	0.110	0.034
FVTX-S ($-2.5 < \eta < -1.5$)	0.232	0.052
FVTX-S ($-3.0 < \eta < -1.0$)	0.274	0.070

three event planes described above are shown in Fig. 3(c), and are consistent between detectors to within 5%(15%) for $v_2(v_3)$ over the whole p_T range.

The main sources of systematic uncertainty for the v_n measurements are (1) track backgrounds from weak decays and photon conversions, (2) multiple ^{3}He + Au collisions in a bunch crossing (pileup), (3) biases in event plane determination, (4) the effect of detector alignment and performance on the v_n measurement, and (5) elementary process or nonflow correlations; we assign the following values to account for these systematic uncertainties. (1) We estimate the track background contribution by reducing the spatial matching windows in PC3 from 3σ to 2σ and find a change of less than 2%(5%) fractionally in $v_2(v_3)$. (2) We expect the v_n from pileup events to be modestly reduced. Conservatively assuming that pileup events that contaminate the sample at the level of 4%–5% have a negligible v_n, this results in a $^{+0}_{-5}$% systematic uncertainty. (3) Event plane effects are estimated from v_n measurements using different event plane detectors as shown in Fig. 3(c). They are no more than 5%(15%) for $v_2(v_3)$. (4) The difference of v_n for charged hadrons measured by the east and west DC arms are found to be less than 2%(15%) for $v_2(v_3)$. (5) The contribution from nonflow correlations at each p_T is estimated from Fig. 3(b), reaching a maximum of 7% (15%) for $v_2(v_3)$. We do not attempt to correct for this contribution and instead treat it as a systematic uncertainty. All of these contributions are summed in quadrature.

The final v_n results are determined using the event plane measured in the FVTX-S covering $-3.0 < \eta < -1.0$, and these are shown in Fig. 4, with the systematic uncertainties as described above. We observe sizable v_2 and v_3 anisotropies that both rise as a function of p_T. It is notable that the $v_2(p_T)$ values for central ^{3}He + Au collisions are very similar within uncertainties with those reported earlier in central d + Au collisions [10]. In scenarios where these anisotropies reflect the initial geometry, this similarity would be expected as the initial eccentricities ε_2 for central d + Au and ^{3}He + Au are essentially identical, as shown in Table I. The same calculations indicate a much larger ε_3 in ^{3}He + Au compared with d + Au collisions. However, the d + Au data used in [10] were taken in 2008, without a central trigger and before the FVTX was installed, and did not allow extraction of a statistically significant v_3 in d + Au.

We now compare the experimental data with theory predictions in the literature. Four such predictions shown in Fig. 4 employ viscous hydrodynamics with η/s at or near the conjectured lower bound $1/4\pi$ [30]. The Glauber + Hydro [31] (IP-Glasma + Hydro [32]) utilize Glauber (IP-Glasma) initial conditions, and both overpredict the magnitude of the v_2 and v_3 data. Improved agreement may be achieved by utilizing a larger value of η/s or by the inclusion of a transition from QGP to a hadronic cascade, which has much larger viscous effects and thus decreases the overall flow. The SONIC calculation [14] employs Glauber

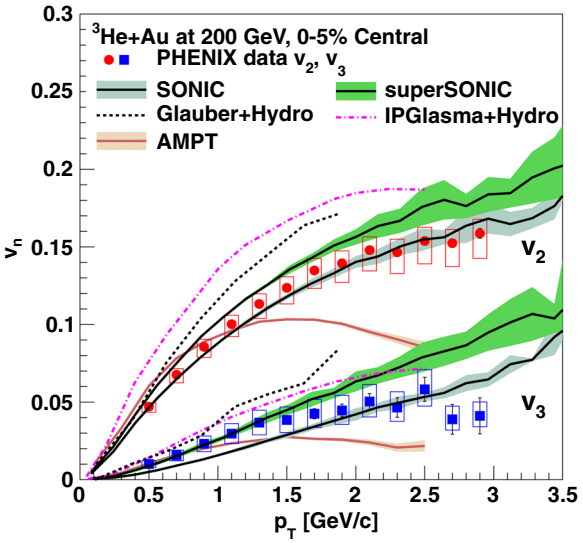

FIG. 4 (color online). Results for v_2 (circles) and v_3 (squares) as a function of p_T for inclusive charged hadrons at midrapidity in 0%–5% central ^{3}He + Au collisions at $\sqrt{s_{NN}} = 200$ GeV; error bars are statistical and shaded bars are systematic uncertainties as described in the text. Also shown are various theoretical calculations, see text for details and references.

initial conditions, viscous hydrodynamics, and then at $T = 170$ MeV, a transition to a hadronic cascade. The SUPERSONIC calculation [33] additionally includes preequilibrium dynamics that boosts the initial velocity fields at the earliest times. The impact of preequilibrium is modest on the v_2 values and both calculations agree with the data within uncertainties. The effect of preequilibrium on v_3 is significantly larger as the triangular flow takes longer to develop [14]. The SUPERSONIC prediction agrees well with the experimental data for $p_T < 1.5$ GeV/c, and then the data trend towards the SONIC prediction at higher p_T.

Lastly, we compare to calculations utilizing the a-multiphase-transport (AMPT) model [34], which incorporates both partonic and hadronic scattering, and has recently been compared with anisotropies in central p + Pb and d + Au collisions [35,36]. AMPT results for ^{3}He + Au agree reasonably with the experimental v_2 and v_3 data for $p_T < 1$ GeV and then significantly underpredict the data. Possible underlying causes of the anisotropies within the AMPT model are discussed in Ref. [37].

We have presented first results on azimuthal anisotropies v_2 and v_3 in central ^{3}He + Au collisions at $\sqrt{s_{NN}} =$ 200 GeV. Calculations including hydrodynamic expansion of the initial hot spots created in ^{3}He + Au collisions qualitatively describe the data. Further comparison with different theoretical models should be informative in terms of the contributions from the initial geometry and each time stage in the medium evolution including preequilibrium. Forthcoming results from p + Au collisions at RHIC will provide a full suite of geometries with highly asymmetric collisions to constrain the origin of the observed anisotropies.

We thank the staff of the Collider-Accelerator and Physics Departments at Brookhaven National Laboratory and the staff of the other PHENIX participating institutions for their vital contributions. We acknowledge support from the Office of Nuclear Physics in the Office of Science of the Department of Energy, the National Science Foundation, a sponsored research grant from Renaissance Technologies LLC, Abilene Christian University Research Council, Research Foundation of SUNY, and Dean of the College of Arts and Sciences, Vanderbilt University (U.S.A), Ministry of Education, Culture, Sports, Science, and Technology and the Japan Society for the Promotion of Science (Japan), Conselho Nacional de Desenvolvimento Científico e Tecnológico and Fundação de Amparo à Pesquisa do Estado de São Paulo (Brazil), Natural Science Foundation of China (People's Republic of China), Ministry of Science, Education, and Sports (Croatia), Ministry of Education, Youth and Sports (Czech Republic), Centre National de la Recherche Scientifique, Commissariat à l'Énergie Atomique, and Institut National de Physique Nucléaire et de Physique des Particules (France), Bundesministerium für Bildung und Forschung, Deutscher Akademischer Austausch Dienst, and Alexander von Humboldt Stiftung (Germany), National Science Fund, OTKA, Károly Róbert University College, and the Ch. Simonyi Fund (Hungary), Department of Atomic Energy and Department of Science and Technology (India), Israel Science Foundation (Israel), Basic Science Research Program through NRF of the Ministry of Education (Korea), Physics Department, Lahore University of Management Sciences (Pakistan), Ministry of Education and Science, Russian Academy of Sciences, Federal Agency of Atomic Energy (Russia), VR and Wallenberg Foundation (Sweden), the U.S. Civilian Research and Development Foundation for the Independent States of the Former Soviet Union, the Hungarian American Enterprise Scholarship Fund, and the US-Israel Binational Science Foundation.

[*]Deceased.
[†]PHENIX Spokesperson.
morrison@bnl.gov
[‡]PHENIX Spokesperson.
jamie.nagle@colorado.edu

[1] U. Heinz and R. Snellings, Collective flow and viscosity in relativistic heavy-ion collisions, Annu. Rev. Nucl. Part. Sci. **63**, 123 (2013).
[2] K. Adcox *et al.* (PHENIX Collaboration), Formation of dense partonic matter in relativistic nucleus-nucleus collisions at RHIC: Experimental evaluation by the PHENIX Collaboration, Nucl. Phys. **A757**, 184 (2005).
[3] J. Adams *et al.* (STAR Collaboration), Experimental and theoretical challenges in the search for the quark gluon plasma: The STAR Collaboration's critical assessment of the evidence from RHIC collisions, Nucl. Phys. **A757**, 102 (2005).
[4] V. Khachatryan *et al.* (CMS Collaboration), Observation of long-range near-side angular correlations in proton-proton collisions at the LHC, J. High Energy Phys. 09 (2010) 091.
[5] S. Chatrchyan *et al.* (CMS Collaboration), Multiplicity and transverse momentum dependence of two- and four-particle correlations in pPb and PbPb collisions, Phys. Lett. B **724**, 213 (2013).
[6] B. B. Abelev *et al.* (ALICE Collaboration), Long-range angular correlations of π, K, and p in p-Pb collisions at $\sqrt{s_{\rm NN}} = 5.02$ TeV, Phys. Lett. B **726**, 164 (2013).
[7] B. Abelev *et al.* (ALICE Collaboration), Long-range angular correlations on the near and away side in p-Pb collisions at $\sqrt{s_{NN}} = 5.02$ TeV, Phys. Lett. B **719**, 29 (2013).
[8] G. Aad *et al.* (ATLAS Collaboration), Measurement of long-range pseudorapidity correlations and azimuthal harmonics in $\sqrt{s_{NN}} = 5.02$ TeV proton-lead collisions with the ATLAS detector, Phys. Rev. C **90**, 044906 (2014).
[9] L. Adamczyk *et al.* (STAR Collaboration), Long-range pseudorapidity dihadron correlations in $d+$Au collisions at $\sqrt{s_{NN}} = 200$ GeV, Phys. Lett. B **747**, 265 (2015).
[10] A. Adare *et al.* (PHENIX Collaboration), Measurement of Long-Range Angular Correlation and Quadrupole Anisotropy of Pions and (anti)Protons in Central $d+$Au Collisions at $\sqrt{s_{NN}} = 200$ GeV, Phys. Rev. Lett. **114**, 192301 (2015).
[11] A. Adare *et al.* (PHENIX Collaboration), Quadrupole Anisotropy in Dihadron Azimuthal Correlations in Central $d+$Au Collisions at $\sqrt{s_{NN}} = 200$ GeV, Phys. Rev. Lett. **111**, 212301 (2013).
[12] P. Bozek, Collective flow in p-Pb and d-Pb collisions at TeV energies, Phys. Rev. C **85**, 014911 (2012).
[13] K. Dusling and R. Venugopalan, Comparison of the color glass condensate to dihadron correlations in proton-proton and proton-nucleus collisions, Phys. Rev. D **87**, 094034 (2013).
[14] J. L. Nagle, A. Adare, S. Beckman, T. Koblesky, J. O. Koop, D. McGlinchey, P. Romatschke, J. Carlson, J. E. Lynn, and M. McCumber, Exploiting Intrinsic Triangular Geometry in Relativistic ^{3}He + Au Collisions to Disentangle Medium Properties, Phys. Rev. Lett. **113**, 112301 (2014).
[15] J.-Y. Ollitrault, Anisotropy as a signature of transverse collective flow, Phys. Rev. D **46**, 229 (1992).
[16] K. Adcox *et al.* (PHENIX Collaboration), PHENIX detector overview, Nucl. Instrum. Methods Phys. Res., Sect. A **499**, 469 (2003).
[17] K. Adcox *et al.* (PHENIX Collaboration), PHENIX central arm tracking detectors, Nucl. Instrum. Methods Phys. Res., Sect. A **499**, 489 (2003).
[18] A. Adare *et al.* (PHENIX Collaboration), Centrality categorization for $R_{p(d)+A}$ in high-energy collisions, Phys. Rev. C **90**, 034902 (2014).
[19] C. Aidala *et al.*, The PHENIX Forward Silicon Vertex Detector, Nucl. Instrum. Methods Phys. Res., Sect. A **755**, 44 (2014).
[20] A. Adare *et al.* (PHENIX Collaboration), Spectra and ratios of identified particles in Au + Au and $d+$Au collisions at $\sqrt{s_{NN}} = 200$ GeV, Phys. Rev. C **88**, 024906 (2013).
[21] A. Adare *et al.* (PHENIX Collaboration), Suppression of back-to-back hadron pairs at forward rapidity in $d+$Au

Collisions at $\sqrt{s_{NN}} = 200$ GeV, Phys. Rev. Lett. **107**, 172301 (2011).

[22] A. Adare *et al.* (PHENIX Collaboration), Nuclear Modification of ψ', χ_c, and J/ψ Production in $d + \mathrm{Au}$ Collisions at $\sqrt{s_{NN}} = 200$ GeV, Phys. Rev. Lett. **111**, 202301 (2013).

[23] C. Loizides, J. Nagle, and P. Steinberg, Improved version of the PHOBOS Glauber Monte Carlo, arXiv:1408.2549v2, code available at http://www.hepforge.org/downloads/tglaubermc.

[24] M. L. Miller, K. Reygers, S. J. Sanders, and P. Steinberg, Glauber modeling in high energy nuclear collisions, Annu. Rev. Nucl. Part. Sci. **57**, 205 (2007).

[25] A. M. Poskanzer and S. A. Voloshin, Methods for analyzing anisotropic flow in relativistic nuclear collisions, Phys. Rev. C **58**, 1671 (1998).

[26] S. S. Adler *et al.* (PHENIX Collaboration), Elliptic Flow of Identified Hadrons in $\mathrm{Au} + \mathrm{Au}$ Collisions at $\sqrt{s_{NN}} = 200$ GeV, Phys. Rev. Lett. **91**, 182301 (2003).

[27] S. S. Adler *et al.* (PHENIX Collaboration), Measurement of Identified π^0 and Inclusive Photon v_2 and Implication to the Direct Photon Production in $\sqrt{s_{NN}} = 200$ GeV $\mathrm{Au} + \mathrm{Au}$ Collisions, Phys. Rev. Lett. **96**, 032302 (2006).

[28] S. Afanasiev *et al.* (PHENIX Collaboration), Systematic studies of elliptic flow measurements in $\mathrm{Au} + \mathrm{Au}$ collisions at $\sqrt{s} = 200$ GeV, Phys. Rev. C **80**, 024909 (2009).

[29] A. J. Baltz, C. Chasman, and S. N. White, Correlated forward-backward dissociation and neutron spectra as luminosity monitor in heavy ion colliders, Nucl. Instrum. Methods Phys. Res., Sect. A **417**, 1 (1998).

[30] P. K. Kovtun, D. T. Son, and A. O. Starinets, Viscosity in Strongly Interacting Quantum Field Theories from Black Hole Physics, Phys. Rev. Lett. **94**, 111601 (2005).

[31] P. Bozek and W. Broniowski, Hydrodynamic modeling of ^{3}He-Au collisions at $\sqrt{s_{NN}} = 200$ GeV, Phys. Lett. B **747**, 135 (2015).

[32] B. Schenke and R. Venugopalan, Collective effects in light-heavy ion collisions, Nucl. Phys. **A931**, 1039 (2014).

[33] P. Romatschke, Light-heavy ion collisions: A window into pre-equilibrium QCD dynamics?, Eur. Phys. J. C **75**, 305 (2015).

[34] Z.-W. Lin, C. M. Ko, B.-A. Li, B. Zhang, and S. Pal, A Multi-phase transport model for relativistic heavy ion collisions, Phys. Rev. C **72**, 064901 (2005).

[35] A. Bzdak and G.-L. Ma, Elliptic and Triangular Flow in $p + \mathrm{Pb}$ and Peripheral $\mathrm{Pb} + \mathrm{Pb}$ Collisions from Parton Scatterings, Phys. Rev. Lett. **113**, 252301 (2014).

[36] J. D. Orjuela Koop, A. Adare, D. McGlinchey, and J. L. Nagle, Long-range azimuthal correlations from parton scattering in central $\mathrm{p} + \mathrm{Au}$, $\mathrm{d} + \mathrm{Au}$, and $^3\mathrm{He} + \mathrm{Au}$ collisions at $\sqrt{s_{NN}} = 200$ GeV, arXiv:1501.06880.

[37] L. He, T. Edmonds, Z.-W. Lin, F. Liu, D. Molnar, and F. Wang, Anisotropic parton escape is the dominant source of azimuthal anisotropy in transport models, arXiv:1502.05572.